

CornViT: A Multi-Stage Convolutional Vision Transformer Framework for Hierarchical Corn Kernel Analysis

Sai Teja Erukude, Jane Mascarenhas and Lior Shamir

Kansas State University

1701 Platt St, Manhattan, KS 66506, USA

erukude.saiteja@gmail.com, jane.mascarenhas.work@gmail.com, lshamir@mtu.edu

Abstract

Accurate grading of corn kernels is critical for seed certification, directional seeding, and breeding, yet it is still predominantly performed by manual inspection. This work introduces CornViT, a three-stage Convolutional Vision Transformer (CvT) framework that emulates the hierarchical reasoning of human seed analysts for single-kernel evaluation. Three sequential CvT-13 classifiers operate on 384×384 RGB images: Stage 1 distinguishes pure from impure kernels; Stage 2 categorizes pure kernels into flat and round morphologies; and Stage 3 determines the embryo orientation (up vs. down) for pure, flat kernels. Starting from a public corn seed image collection, we manually relabeled and filtered images to construct three stage-specific datasets: 7265 kernels for purity, 3859 pure kernels for morphology, and 1960 pure-flat kernels for embryo orientation, all released as benchmarks. Head-only fine-tuning of ImageNet-22k pretrained CvT-13 backbones yields test accuracies of 93.76% for purity, 94.11% for shape, and 91.12% for embryo-orientation detection. Under identical training conditions, ResNet-50 reaches only 76.56 to 81.02 percent, whereas DenseNet-121 attains 86.56 to 89.38 percent accuracy. These results highlight the advantages of convolution-augmented self-attention for kernel analysis. To facilitate adoption, we deploy CornViT in a Flask-based web application that performs stage-wise inference and exposes interpretable outputs through a browser interface. Together, the CornViT framework, curated datasets, and web application provide a deployable solution for automated corn kernel quality assessment in seed quality workflows. Source code and data are publicly available.

1 Introduction

Maize (*Zea mays*) is a major global cereal crop used for food, feed, and bioenergy, and its kernel quality strongly influences germination, early vigor, and final yield. Kernel attributes such as physical purity, damage, and varietal consistency also affect downstream processes, including milling, grain fractionation, and industrial applications Nehoshtan et al. (2021). High standards of purity and kernel quality have been established by seed certification programs. However, the qualitative standards are still largely determined through a manual process that involves trained personnel inspecting, counting, and sorting kernels Ghaffari (2024). The current processes of evaluating kernels are time-consuming, resource-intensive, and cannot be easily scaled to meet the demands of modern high-throughput breeding and commercial seed production. As a result, there is growing interest in automation, particularly using machine vision and deep learning techniques, to assist in automated seed evaluation and processing. That includes kernel counting, kernel defect detection, kernel breakage estimation, and seed vigor assessment.

Machine vision Sonka et al. (2013) and deep learning LeCun et al. (2015) have rapidly advanced kernel-level inspection by providing scalable alternatives to manual evaluation. Early systems relied on handcrafted shape and texture descriptors paired with classical classifiers to distinguish whole from broken kernels or to assess purity. With modern deep learning, CNN-based O’shea and Nash (2015) models have been developed for tasks such as on-ear kernel detection and counting, high-throughput phenotyping, and classification of good, defective,

and impurity kernels Velesaca et al. (2020). The results demonstrated that deep feature extractors can match or surpass human graders on specific tasks. Self-supervised and contrastive learning approaches further reduce annotation costs by learning transferable kernel representations that support embryo-orientation detection and segmentation. At the same time, hyperspectral and RGB-based models have been used to predict maize variety, vigor, and germination Dong et al. (2023). These studies collectively establish that image-based deep learning can capture many aspects of seed and kernel quality and form a strong foundation for automation.

Despite these advances, current image-based kernel analysis methods still face several major challenges. First, most rely on a single, monolithic classifier that maps directly from an image to a composite label such as “good”, “defective”, or “impurity”. This compresses diverse visual cues, purity, morphology, and orientation into one decision, making error analysis difficult, and provides limited interpretability for agronomists and seed analysts. Second, the field remains dominated by CNN-based and hand-crafted feature pipelines that are effective for local pattern extraction but less suited to capturing the global shape context and subtle structural cues needed to distinguish borderline impurities or embryo orientation. Finally, many prior works address only one sub-task at a time (e.g., purity or embryo orientation) or are tightly coupled to specific imaging setups, which complicates reuse across quality dimensions or deployment environments. Although Vision Transformers (ViTs) Dosovitskiy (2020) and related architectures offer improved capacity for modeling long-range relationships and have shown strong performance in plant disease detection and phenotyping Zhou et al. (2021), their use for fine-grained, kernel-level evaluation is still limited. In contrast, human graders naturally follow a structured, multi-stage reasoning process: they begin by assessing whether a kernel is pure, then determine its morphological category, and finally examine its orientation and finer anatomical features. Emulating this hierarchical decision pathway in automated models helps address both interpretability and modeling limitations in prior work.

At the same time, there is a broader trend toward deep learning-based image analysis in precision agriculture, which further motivates our approach. In crop-weed management, CWRepViT-

Net has shown that encoder-decoder frameworks built from RepViT blocks can perform accurate semantic segmentation of crops and multiple weed species throughout the life cycle of soybean fields, highlighting the potential of transformer-style backbones for fine-grained canopy understanding and decision support in the field Gomroki et al. (2025). In aerial monitoring, Succulent-YOLO combines a CLIP-enhanced YOLOv10 detector, dynamic group convolutions, and a multi-scale fusion neck with a Mamba-based super-resolution module (MambaIR) to detect succulent plants in UAV imagery, achieving high mean average precision even on low-resolution inputs Li et al. (2025). Closer to our application domain, Rocha et al. developed a real-time system that mounts a camera on a self-propelled forage harvester to capture images of chopped corn silage and uses machine learning to count whole kernels and estimate the Kernel Processing Score with strong agreement to laboratory sieve analysis, demonstrating that image-based models can provide actionable quality metrics directly in harvesting equipment Rocha et al. (2022). Together, these examples show that deep learning, including transformer-based and CLIP-enhanced architectures, is increasingly used to automate image-based assessment of crops and grain products at canopy, field, and processing levels.

In this study, we investigate whether multi-stage Convolutional Vision Transformers (CvTs) Wu et al. (2021b) can model the hierarchical decision-making process used by human seed analysts for single-kernel evaluation. To this end, we introduce CornViT, a three-step CvT-based framework that sequentially classifies kernel purity, morphological type, and embryo orientation. Each stage employs an independently fine-tuned CvT-13 model Wu et al. (2021c) operating on 384×384 RGB images, leveraging CvT’s combination of convolutional inductive biases with the global context modeling of Transformers. By decomposing grading into three explicit decisions and using a transformer-based backbone, CornViT is designed to address the limitations of prior work: it replaces monolithic labels with interpretable intermediate outputs, uses convolution-augmented self-attention to capture both local surface cues and global kernel shape, and provides modular stages that can be adapted to different imaging setups or extended to additional quality attributes. Across the three

stages, CornViT substantially outperforms strong CNN baselines: ResNet-50 He et al. (2016); Koonce (2021) attains only around 77 to 81 percent accuracy and DenseNet-121 Huang et al. (2017) around 87 to 89 percent, whereas CornViT achieves 93.76%, 94.11%, and 91.12% test accuracy for purity, shape, and embryo-orientation classification, respectively. This highlights the advantages of transformer-based architectures for fine-grained agricultural vision tasks. We deploy the models in a lightweight web application that supports stage-wise inference and exposes interpretable outputs through a simple browser interface, illustrating how such a framework can be integrated into seed-quality and precision-agriculture workflows.

Three major contributions from this research are as follows:

1. Introduction of CornViT, a three-stage CvT-based framework that mirrors human-style hierarchical reasoning for kernel purity, morphology, and embryo orientation.
2. Construction and release of a stage-wise annotated corn kernel dataset comprising three curated subsets aligned with the purity, shape, and embryo-orientation tasks.
3. Development of a ready-to-use web application that exposes the full CornViT pipeline through a browser interface, enabling easy adoption in seed quality assessment and precision-agriculture workflows.

The remainder of this paper describes related work (Section 2), materials and methods (Section 3), experimental results (Section 4), the web application integration (Section 5), a detailed discussion (Section 6), and conclusions (Section 7).

2 Background and Related Work

2.1 Automated Inspection of Maize Kernels and Seeds

Within this space, several studies have focused specifically on corn and other crop seeds. Liao et al. developed an early machine vision system

for automated corn quality inspection in which binary images of kernels were converted into one-dimensional shape profiles; key shape parameters were then extracted and fed into a neural network. Their model accurately distinguished whole from broken kernels, achieving up to 99% accuracy for whole kernels and up to 96% for broken kernels Liao et al. (1993). More recently, Qingzhen Zhu et al. presented a hyperspectral imaging-based maize variety identification approach that combines SG and SNV preprocessing, CARS wavelength selection, and a CNN-LSTM model, achieving 95.27% accuracy and outperforming traditional chemometric methods, demonstrating its effectiveness for efficient and reliable maize variety classification Zhu et al. (2025).

Related ideas have also been applied to other crops. For example, Prashant Yawalkar and colleagues developed an automated onion seed quality assessment system using image processing and machine learning, showing that CNN-based deep learning outperforms traditional methods in both accuracy and scalability, and providing a faster, more reliable alternative to manual inspection for precision agriculture Surse and Yawalkar (2025).

More recent work has explored modern representation learning for maize kernel tasks. David Dong demonstrated that self-supervised contrastive learning methods (NNCLR and SimCLR) Chen et al. (2020) enable highly efficient maize kernel embryo-orientation classification and segmentation, outperforming supervised baselines, transferring effectively across tasks, and achieving strong accuracy (DICE 0.81) even with as little as 1% annotated data Dong et al. (2023). These results indicate that kernel-level inspection tasks are well-suited to contemporary deep and representation-learning pipelines.

2.2 Embryo Orientation and Directional Seeding

Seed orientation plays a significant role in optimizing corn growth and yield, as several studies have shown that directing seeds during planting can influence leaf azimuth, canopy structure, and ultimately light interception. Peters and Woolley (1959) first noted that seed direction affects leaf orientation Peters and Woolley (1959), and Fortin and Pierce (1996) demonstrated that controlled seed orientation can align a majority of ear leaves with embryo

direction Fortin and Pierce (1996). Field trials by Toler et al. (1999) further showed that manipulating seed orientation to achieve across-row leaf alignment increased yields by 10 to 20 percent by improving light interception and reducing competition Toler et al. (1999). Similarly, Torres et al. (2011) reported that specific seed placements, such as tips down or embryos up, promoted favorable leaf orientation and significantly enhanced light interception and yield Torres et al. (2011).

Motivated by these agronomic benefits, several imaging-based systems have been proposed to automatically determine and adjust embryo orientation. Yingbiao Wang introduced a color-based image processing and contour-analysis method that automatically identifies maize seed embryo orientation with over 95% accuracy and an average error of 2.2° across three maize varieties Wang et al. (2014). Huijuan Bai et al. developed an identification and adjustment prototype that orients corn seeds with the embryo side upward and the long axis perpendicular to the row, using image processing and pneumatic adjustment to achieve an 84% success rate in seed orientation Bai et al. (2024). Liu Changqing et al. proposed another image-based method that detects the embryo by its whitish color and position along the major axis, then determines tip direction to calculate the orientation angle, achieving 97.1% accuracy Changqing et al. (2015). These systems typically rely on handcrafted geometric and color-based features within device-specific imaging setups, which can make them sensitive to variations in lighting, seed appearance, and camera conditions.

More recently, David Dong’s work on self-supervised contrastive learning showed that representation-learning approaches can further improve data efficiency and robustness for embryo-orientation classification and segmentation Dong et al. (2023). In contrast to handcrafted pipelines, our CornViT framework adopts a multi-stage Vision Transformer architecture that autonomously learns hierarchical features, explicitly mirrors the purity–shape–orientation decision sequence used by human graders, and aims to provide a more robust, accurate, and scalable system for modern seed phenotyping and directional seeding applications.

2.3 Vision Transformers in Precision Agriculture

Transformers are increasingly being adopted in agriculture and plant phenotyping, with many recent studies showing that Vision Transformers (ViTs) and their variants often match or surpass CNNs in tasks such as disease detection, weed identification, and crop monitoring.

In the GreenViT framework, ViTs were used for plant disease detection by dividing images into sequential patches, achieving superior performance compared to state-of-the-art CNN models on benchmark datasets Perez et al. (2023). A ViT-based smartphone application, ViT-SmartAgri, was developed to classify 10 tomato disease classes from 10,010 leaf images, achieving 90.99% accuracy and outperforming Inception V3, demonstrating its potential for large-scale smart agriculture Barman et al. (2024). Guoqiang Li et al. employed a lightweight MobileViT architecture enhanced with inverted residual blocks and a CBAM attention module to efficiently capture long-range dependencies and focus on relevant features, enabling accurate, real-time plant disease detection on mobile devices Li et al. (2023). A ViT-B16 backbone has also been applied to multispectral plant images for disease identification and classification, achieving the highest performance among tested models and highlighting its potential for improving crop disease management De Silva and Brown (2023). Likewise, a ViT model applied to the DeepWeeds dataset achieved 96.9% accuracy across nine weed species, demonstrating the effectiveness of transformer-based architectures for weed detection in agricultural settings Hasasneh et al. (2025).

A recent review by Zhang et al. highlights a broader shift from CNN-only approaches toward ViT and hybrid CNN-transformer models for pest and disease detection, emphasizing that transformer-based architectures offer enhanced global reasoning and feature representation Zhang et al. (2025). Despite these advances, the use of ViTs in seed and kernel quality assessment remains limited, as most studies still depend on CNN-based approaches. This emerging evidence from canopy- and leaf-level tasks nonetheless motivates exploring ViT-style models for fine-grained, kernel-level analysis, such as in the present work.

2.4 Multi-Stage and Hierarchical Deep Learning Pipelines

The concept of multi-stage classification pipelines has been applied in several domains where complex decisions are naturally hierarchical. For example, in cancer grading, a study on Gleason system grading employed a multi-stage deep learning pipeline with multilevel binary CNN classifiers to progressively identify Gleason patterns, scores, and grade groups from digitized prostate biopsy images, demonstrating the effectiveness of staged classification in complex image analysis tasks Hammouda et al. (2022). In a different context, short-term wind power forecasting has been tackled with a multi-stage, hierarchical, deep learning pipeline that uses layered information-fusion modules to progressively integrate homogeneous and heterogeneous SCADA data, improving the model’s ability to capture complex temporal and spatial relationships and enhancing prediction accuracy Qin et al. (2025).

More broadly, hierarchical and cascade classifiers have long been used in machine vision applications that require separating easy from difficult examples, identifying subcategories based on specific object characteristics (e.g., morphology), or implementing coarse-to-fine recognition strategies. However, such structured model hierarchies are still rare in seed and kernel inspection, even though expert humans naturally use hierarchical decision processes in this field, for example, first determining whether a sample is pure or impure, then assessing its morphology, and finally examining its orientation and finer anatomical cues.

CornViT extends these ideas to corn kernel grading with a three-stage, task-specific design that explicitly mirrors this human reasoning sequence. Each stage is implemented with a CvT-based architecture, allowing the framework to leverage convolution-augmented self-attention for both local texture analysis and global shape reasoning.

3 Materials and Methods

3.1 Problem Formulation

This study considers single-kernel RGB images in which each image contains exactly one corn kernel on a uniform background. The goal is to obtain a

hierarchical description of the kernel through three binary decisions:

1. Purity (Stage 1):
 - Pure: visually acceptable kernels without obvious defects or discoloration.
 - Impure: kernels that are broken, discolored, silkcut (intact kernels with visible surface cracks and silk-embedded fissures), or otherwise unsuitable.
2. Shape (Stage 2, conditioned on purity):
 - Flat: kernels with a flattened dorsal-ventral profile.
 - Round: kernels with a more equiaxed or rounded morphology.
3. Embryo orientation (Stage 3, conditioned on purity and flat shape):
 - Embryo up: the embryo side faces the camera.
 - Embryo down: the embryo faces away from the camera.

Let $\mathbf{x} \in \mathbb{R}^{H \times W \times 3}$ denote an RGB kernel image, and let f_1, f_2, f_3 denote the Stage 1–3 models. The overall pipeline maps

$$\mathbf{x} \mapsto (y_1, y_2, y_3),$$

where $y_1 \in \{\text{pure, impure}\}$, $y_2 \in \{\text{flat, round}\}$ (if defined), $y_3 \in \{\text{embryo up, embryo down}\}$ (if defined).

For kernels that are predicted as impure in Stage 1, no further classification is attempted, so y_2 and y_3 remain undefined. Similarly, for kernels that are pure but round, Stage 3 is skipped and y_3 is undefined.

In practice, this hierarchy is implemented using three independent binary classifiers, each trained on a stage-specific dataset: D_1 for purity, D_2 for shape (pure kernels only), and D_3 for embryo orientation (pure–flat kernels only). This design allows each stage to specialize in its own decision boundary while maintaining a simple and interpretable global pipeline.

The overall workflow of the proposed CornViT framework is summarized in the flowchart in Figure 1. Starting from a single-kernel RGB image

on a uniform background, the image is first passed through a standardized preprocessing pipeline (resize, augmentation, and ImageNet-style normalization). The preprocessed image is then processed sequentially by three CvT-13 classifiers corresponding to Stage 1 (purity), Stage 2 (shape), and Stage 3 (embryo orientation). At each stage, a binary decision is made, and the hierarchy either terminates (for impure or pure-round kernels) or progresses to the next classifier (for pure and pure-flat kernels). The final output is a hierarchical label tuple (y_1, y_2, y_3) that describes purity, morphology, and embryo orientation, with undefined components for skipped stages.

3.2 Dataset Preparation

A publicly available corn seed image dataset sethu123123 (2025) hosted on Kaggle served as the starting point for this study. The original dataset contains four labeled classes: broken, discolored, pure, and silkcutf, but closer inspection revealed substantial inconsistencies between the class labels and corresponding images. Several images were misplaced across folders and did not correctly represent their annotated class.

Moreover, the predefined class structure did not align with the hierarchical purity, shape, and embryo-orientation objectives considered here. Due to these inconsistencies, the dataset was unsuitable for direct model training. Furthermore, publicly available image datasets for corn kernel analysis are extremely limited, particularly for classification tasks involved in this study.

To address this gap, we performed a comprehensive manual curation process in which each image was visually inspected, hand-picked, and reassigned to its correct class. In total, 17,801 single-kernel images from the Kaggle download were examined. Of these, 10,536 images were duplicates and were therefore discarded. A total of 7265 images were retained in the curated pool used to construct the stage-wise datasets (Tables 1–3). Approximately 50% of these retained images required relabeling their class during curation.

Using this cleaned pool of images, we then constructed three progressively filtered datasets, each tailored to a specific stage of the CornViT pipeline. We regard these three curated datasets as a key contribution of this work. They provide a ready-to-use

benchmark suite for researchers interested in corn kernel purity, morphology, and embryo orientation. The full datasets, along with train/validation/test splits, will be made publicly available at <https://doi.org/10.5281/zenodo.17693853>.

3.2.1 Stage 1 Dataset: Purity Classification

The first stage aims to distinguish pure kernels from impure ones. To this end, the curated dataset was reorganized into two classes: (1) Pure: kernels that are visually free from defects or discoloration, (2) Impure: an aggregated class combining broken, discolored, and silkcutf kernels. Figure 2 presents sample images, and Table 1 summarizes the train/validation/test partitioning, which follows a 70/15/15 split.

Table 1: Summary of the Stage 1 dataset, showing the number of pure and impure samples in the training, validation, and test subsets.

Subset	Pure	Impure	Total
Training Set	2586	2499	5085
Validation Set	555	535	1090
Test Set	554	536	1090
Overall Total	3695	3570	7265

3.2.2 Stage 2 Dataset: Morphological Classification

The second stage focuses on morphological categorization of kernels based on shape characteristics. Since impure kernels are not relevant for further morphological or orientation analysis, only the pure samples from Stage 1 were included in Stage 2. From these, two new classes were identified: (1) Flat and (2) Round. This refinement is motivated by the observation that embryo orientation, the target of Stage 3, is only visually meaningful for flat kernels. Figure 3 presents sample images, and Table 2 summarizes the train/validation/test split.

3.2.3 Stage 3 Dataset: Embryo Orientation Classification

The final stage addresses embryo orientation detection, which is critical for kernel viability and

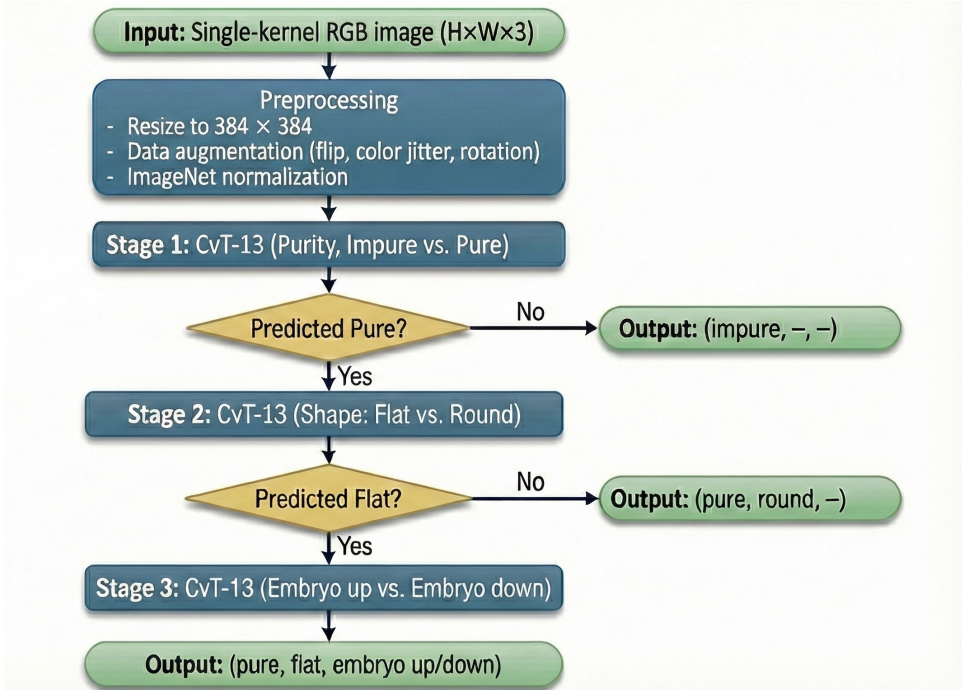


Figure 1: The overall workflow of the proposed CornViT system illustrates how a single-kernel RGB image passes through the preprocessing module and then sequentially through three CvT-13 classifiers.



Figure 2: A sample of images randomly picked from the Stage 1 dataset, showing pure kernels on the left and impure kernels on the right.

Figure 3: Representative samples from the Stage 2 dataset showing flat kernels on the left and round kernels on the right.

3.3 Image Preprocessing

downstream seed processing. Because embryo orientation is visible only on flat kernels, Stage 3 uses the flat subset of the Stage 2 dataset as its base. Two classes were manually derived: (1) Embryo Up and (2) Embryo Down. Figure 4 presents sample images, and Table 3 summarizes the train/validation/test split.

All images were processed through a standardized preprocessing pipeline before being fed into the CornViT models. Each image was first resized to a fixed resolution of 384×384 to match the CvT-13 backbone configuration.

To improve model robustness and mitigate overfitting, we applied a set of common on-the-fly data

Table 2: Summary of the Stage 2 dataset, showing the number of flat and round samples in the training, validation, and test subsets following the 70/15/15 split.

Subset	Flat	Round	Total
Training Set	1374	1329	2703
Validation Set	294	284	578
Test Set	294	284	578
Overall Total	1962	1897	3859

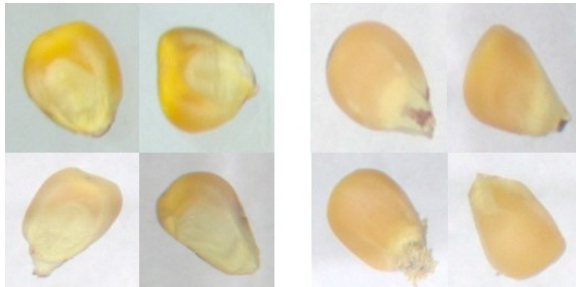


Figure 4: Sample images randomly picked from the Stage 3 dataset depicting embryo orientation, with kernels exhibiting the embryo-up class on the left and the embryo-down class on the right.

augmentations during training. These augmentations included random horizontal and vertical flips, color jittering (adjustments to brightness, contrast, and saturation), and small in-plane rotations of up to 15° . After augmentation, each image was converted into a normalized PyTorch tensor. Normalization followed the standard ImageNet statistics (mean = [0.485, 0.456, 0.406], standard deviation = [0.229, 0.224, 0.225]), which is typically used for models pretrained on ImageNet.

Overall, this preprocessing and augmentation pipeline ensures consistent image scaling, improves generalization under modest domain shifts, and provides well-conditioned inputs for all three CornViT stages. The full implementation is available in the accompanying code repository <https://github.com/SaiTeja-Erukude/CornViT> (accessed on 19 December 2025).

3.4 CornViT Architecture

Each stage of the CornViT framework is implemented as an independent Convolutional Vision

Table 3: Summary of the Stage 3 dataset, showing the number of embryo-up and embryo-down samples in the training, validation, and test subsets following the 70/15/15 split.

Subset	Embryo Up	Embryo Down	Total
Training	813	561	1374
Validation	174	119	293
Test	174	119	293
Total	1161	799	1960

Transformer (CvT-13) classifier Wu et al. (2021b) built on top of the official Microsoft CvT implementation. All three stages share the same backbone architecture but are trained with their own binary classification heads and datasets.

3.4.1 Convolutional Vision Transformer (CvT-13)

The Convolutional Vision Transformer (CvT) Wu et al. (2021b) is a hybrid vision backbone that combines the global self-attention of Vision Transformers (ViTs) Dosovitskiy (2020) with the local inductive biases of CNNs. CvT introduces two key modifications to the vanilla ViT architecture: (1) Convolutional token embedding and (2) Convolutional projection in self-attention.

Instead of partitioning the image into non-overlapping patches and flattening them with a linear projection (as in ViT), CvT uses convolutional layers to generate tokens. These convolutions define local receptive fields and perform spatial down-sampling, allowing each stage to operate on progressively coarser yet semantically richer feature maps. This injects CNN-like properties such as shift, scale, and distortion invariance into the transformer.

In the transformer blocks, CvT replaces pure linear projections for queries, keys, and values with convolutional projections. This enables the attention mechanism to be aware of local spatial neighborhoods while still modeling long-range dependencies through multi-head self-attention. As a result, CvT can better capture fine-grained textures (e.g., kernel surface cues) and global shape simultaneously, often with fewer parameters and FLOPs than comparable ViT or deep CNN backbones.

CvT-13 is the smallest variant described by Wu

et al., with three transformer stages of increasing channel width and decreasing spatial resolution as depicted in Figure 5. For 384×384 inputs, the final stage produces a compact global representation that feeds a lightweight classification head. This makes CvT-13 a good fit for our single-kernel classification setting, where both local surface detail and global kernel morphology are important.

A block-level overview of the proposed CornViT network is shown in Figure 6, which details the internal structure of a single stage: three transform stages of the CvT backbone, followed by a global pooling module and a 2-unit stage-specific classification head. All stages of CornViT follow the same internal structure.

3.4.2 Experimental Setup

All stages in the proposed framework are implemented using the official Microsoft CvT codebase Wu et al. (2021c) with the CvT-13 configuration for 384×384 inputs. For each stage, we initialize a CvT-13 backbone from the publicly available ImageNet-22k pretrained checkpoint Wu et al. (2021a) and adapt it to the corresponding binary task by attaching a 2-unit classification head. Low-level configuration details (e.g., repository cloning and config files) follow the official implementation and are documented in the public code repository.

We adopt a head-only fine-tuning strategy in which the CvT backbone remains frozen and only the final linear classification layer is updated. This choice was motivated by three factors: (i) the curated stage-specific datasets are relatively small compared with large-scale vision corpora, increasing the risk of overfitting when unfreezing deeper transformer blocks; (ii) head-only tuning substantially reduces training time and GPU memory requirements, enabling fully independent training for the three stages; (iii) freezing the backbone ensures stable, comparable feature representations across purity, morphology, and embryo-orientation tasks. Although partial unfreezing (e.g., unfreezing the final transformer stage) may offer additional performance gains—particularly for the visually subtle Stage 3 embryo-orientation task—we leave this investigation for future work.

All stages share the same training configuration, including optimizer, learning-rate scheduler, label smoothing, and number of epochs; the full set of

hyperparameters is summarized in Table 4. The entire training and inference pipeline is implemented in PyTorch (version 2.9.0) Paszke et al. (2019), and the complete source code is publicly available at: <https://github.com/SaiTeja-Erukude/CornViT> (accessed on 19 December 2025).

3.5 Algorithms

The full training and inference procedures of the proposed CornViT framework are summarized using two stage-wise algorithms. Algorithm 1 describes the independent training strategy for each classification stage, and Algorithm 2 outlines the hierarchical inference pipeline used to obtain the final kernel labels.

For clarity, we recall that D_1 , D_2 , and D_3 denote the three curated datasets used in this work: D_1 contains all kernels used for purity classification; D_2 is a subset of D_1 that contains only kernels labeled as pure and is used for shape classification; and D_3 is a subset of D_2 that contains only pure-flat kernels and is used for embryo-orientation classification.

3.6 Evaluation Metrics

To comprehensively assess the performance of each stage in the proposed CornViT framework, we employ standard classification metrics, including Accuracy (Acc), Precision (Pre), Recall (Re), F1 score, and their macro and weighted averages. Since each stage is formulated as a binary classification problem, these metrics characterize different aspects of the model’s behavior, such as overall correctness, reliability on the positive class, and robustness under class imbalance Juba and Le (2019).

Let TP, FP, TN, and FN denote the number of true positives, false positives, true negatives, and false negatives, respectively.

The Accuracy measures the overall proportion of correctly classified samples.

$$\text{Acc} = \frac{\text{TP} + \text{TN}}{\text{TP} + \text{TN} + \text{FP} + \text{FN}} \quad (1)$$

Precision measures the proportion of predicted positive samples that are actually positive.

$$\text{Pre} = \frac{\text{TP}}{\text{TP} + \text{FP}} \quad (2)$$

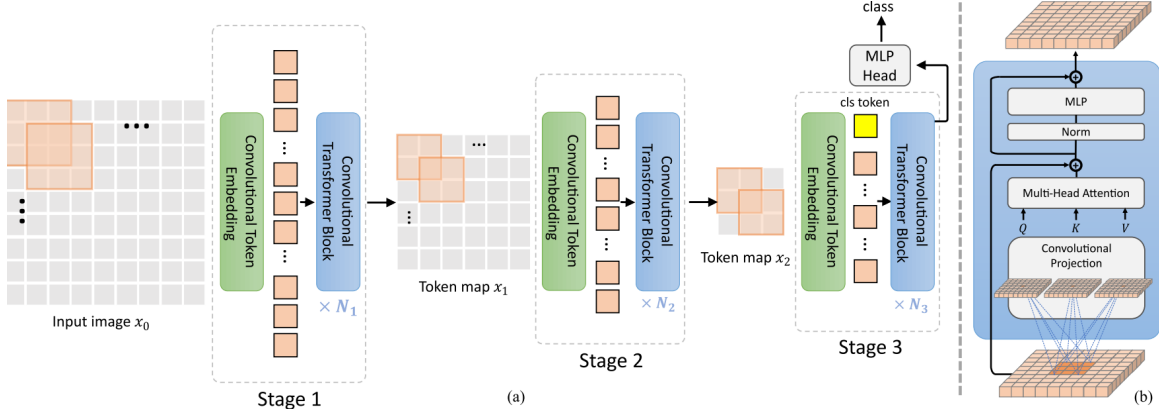


Figure 5: Schematic of the CvT-13 architecture used as the backbone in all CornViT stages Wu et al. (2021b). (a) The complete architecture highlights the hierarchical multi-stage design facilitated by the Convolutional Token Embedding layer. (b) A detailed illustration of the Convolutional Transformer Block, which begins with a convolutional projection layer.

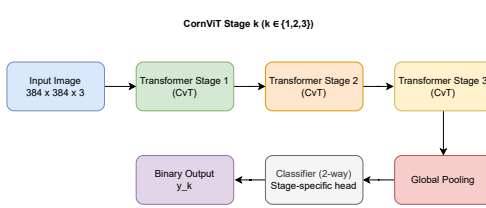


Figure 6: Block diagram of the proposed CornViT network showing internal structure of a single stage.

Recall (also known as sensitivity) quantifies the proportion of actual positive samples that are correctly identified.

$$Re = \frac{TP}{TP + FN} \quad (3)$$

The F1 score is the harmonic mean of Precision and Recall.

$$F1 = 2 \cdot \frac{Pre \cdot Re}{Pre + Re} \quad (4)$$

For completeness, we also report macro and weighted averages across classes. Let C be the number of classes (here, $C = 2$), and let Pre_c , Re_c , and $F1_c$ denote the class-wise metrics for class c , with n_c samples in class c and $N = \sum_{c=1}^C n_c$ the total number of samples.

The macro-average of a generic metric M is

$\{Pre, Re, F1\}$ is computed as

$$M_{\text{macro}} = \frac{1}{C} \sum_{c=1}^C M_c, \quad (5)$$

which treats all classes equally.

The weighted-average version accounts for class imbalance by weighting each class by its support:

$$M_{\text{weighted}} = \sum_{c=1}^C \frac{n_c}{N} M_c. \quad (6)$$

In our experiments, we report Accuracy together with macro- and weighted-average Precision, Recall, and F1, providing a balanced view of performance under potentially imbalanced class distributions at each CornViT stage. Model selection for each stage is based primarily on validation Accuracy, while also inspecting macro- and weighted-average F1; when candidate models achieve similar validation Accuracy, we prefer those with higher macro-F1 to avoid degrading minority-class performance.

4 Results

4.1 Baseline CNNs

To establish performance benchmarks and contextualize the performance of the proposed CornViT framework, baseline experiments were carried out.

Table 4: Summary of training configuration for all CornViT stages.

Component	Setting
Backbone	CvT-13 (official Microsoft implementation) Wu et al. (2021c)
Input resolution	384 × 384
Number of classes	2 (binary classification)
Pretrained weights	ImageNet-22k checkpoint (OneDrive link) Wu et al. (2021a)
Fine-tuning strategy	Head-only (backbone frozen)
Optimizer	AdamW Loshchilov and Hutter (2017)
Learning rate	1×10^{-4}
Weight decay	0.05
Loss function	SoftTargetCrossEntropy
Label smoothing	0.1
Learning-rate scheduler	CosineLRScheduler
Warm-up	5 epochs, <code>warmup_lr_init = 1×10^{-5}</code>
Minimum LR	1×10^{-6}
Total epochs	20
Implementation	PyTorch Paszke et al. (2019)
Repository	https://github.com/SaiTeja-Erukude/CornViT

Two convolutional neural networks (CNNs) O’shea and Nash (2015) were utilized: ResNet-50 He et al. (2016); Koonce (2021) and DenseNet-121 Huang et al. (2017). Both models were chosen because they represent strong, well-established backbones for image classification and have been extensively used in agricultural and plant-phenotyping tasks.

A broader survey including additional lightweight CNNs such as EfficientNet or MobileNet would be valuable, but lies outside the scope of this study. Our goal in this work is not to exhaustively benchmark all CNN variants, but rather to compare a representative pair of strong, widely used CNN backbones against the proposed multi-stage CvT framework on a newly curated kernel dataset. Exploring a broader range of mobile-oriented CNNs is therefore left as complementary future work, orthogonal to the main question of whether CvT offers advantages for hierarchical kernel-level analysis.

ResNet-50 is a 50-layer residual network that introduces identity-based skip connections (residual blocks) to ease the optimization of deep models and mitigate vanishing-gradient issues. Each residual block learns a residual mapping with respect to its input, allowing gradients to flow more directly through the network and enabling effective training of very deep architectures Koonce (2021).

DenseNet-121 is a densely connected convolutional network in which each layer receives, as input,

the concatenation of all feature maps from preceding layers within the same dense block. This design encourages feature reuse, improves information flow, and reduces the number of parameters compared to traditional feed-forward CNNs with comparable depth Huang et al. (2017).

For all three CornViT stages (purity, shape, embryo orientation), the baselines were configured as follows:

- Both ResNet-50 and DenseNet-121 were initialized from ImageNet-pretrained weights.
- The final classification layers were replaced with new 2-class fully connected heads, matching the binary tasks at each stage.
- The same preprocessing and data augmentation pipeline described in Section 3.3 was applied (resize, random flips, color jitter, small rotations, and ImageNet normalization), ensuring that differences in performance were attributable primarily to the backbone architecture rather than to differing data pipelines.
- Training was performed using binary cross-entropy loss and Adam optimizer. The number of epochs, batch size, and learning-rate schedule were kept comparable to those used for the CvT models to provide a fair comparison.

Algorithm 1 CornViT Stage-wise Training

Require:

```
1:  $D_1 = \{(x_i, y_i^1)\}$ : Stage 1 data (impure vs. pure)
2:  $D_2 = \{(x_j, y_j^2)\}$ : Stage 2 data (flat vs. round; pure only)
3:  $D_3 = \{(x_k, y_k^3)\}$ : Stage 3 data (embryo up vs. down; pure–flat only)
4: CvT-13 models  $f_1, f_2, f_3$  with 2-class heads
5: train_transforms, val_transforms, number of epochs  $T = 20$ 
6: for  $s \in \{1, 2, 3\}$  do ▷ stage-wise training loop
7:   Initialize  $f_s$  with ImageNet-pretrained CvT-13 weights
8:   Replace final classification head with a 2-unit linear layer
9:   Freeze all backbone parameters of  $f_s$  (head-only fine-tuning)
10:  if  $s = 1$  then
11:     $D_s \leftarrow D_1$ 
12:  else if  $s = 2$  then
13:     $D_s \leftarrow D_2$ 
14:  else
15:     $D_s \leftarrow D_3$ 
16:  end if
17:  for epoch = 1 to  $T$  do
18:    for all  $(x, y)$  in training split of  $D_s$  do
19:       $x_{\text{aug}} \leftarrow \text{train\_transforms}(x)$ 
20:       $p \leftarrow f_s(x_{\text{aug}})$ 
21:       $L \leftarrow \text{SoftTargetCrossEntropy}(p, y)$ 
22:      Update head parameters of  $f_s$  using AdamW to minimize  $L$ 
23:    end for
24:    Evaluate  $f_s$  on the validation split of  $D_s$  using val_transforms
25:  end for
26: end for
```

- The train/validation/test splits were also the same as the corresponding CornViT models to ensure a fair comparison.

Results from Table 5 confirm that DenseNet-121 provides a stronger baseline than ResNet-50 across all three tasks, likely due to its enhanced feature reuse and gradient flow. Nevertheless, the proposed CvT-based CornViT models achieve higher accuracies in all stages (93.76%, 94.11%, and 91.12%, respectively), highlighting the benefit of transformer-based global reasoning and the hierarchical design for fine-grained kernel classification.

4.2 Stage 1—Pure vs. Impure Classification

Stage 1 distinguishes impure from pure kernels across 1090 test images. Table 6 summarizes per-class metrics, and the corresponding confusion ma-

Table 5: Baseline accuracies of ResNet-50 and DenseNet-121 on the same test sets used for CornViT evaluation.

Stage	ResNet-50	DenseNet-121
Stage 1	76.56%	86.56%
Stage 2	78.21%	87.05%
Stage 3	81.02%	89.38%

trix is shown in Figure 7. Performance is well-balanced across classes, with both pure and impure kernels achieving F1 scores above 0.93. This is important in practice: false positives (impure labeled as pure) can contaminate subsequent grading, while false negatives (pure labeled as impure) reduce usable yield. The symmetry of Precision and Recall suggests that CornViT Stage 1 maintains a good trade-off between sensitivity and specificity.

Table 6: Classification report for Stage 1 (Impure vs. Pure).

Class	Precision	Recall	F1-Score	Support
Pure	0.9370	0.9404	0.9387	554
Impure	0.9382	0.9347	0.9365	536
Accuracy	—	—	0.9376	1090
Macro avg	0.9376	0.9375	0.9376	1090
Weighted avg	0.9376	0.9376	0.9376	1090

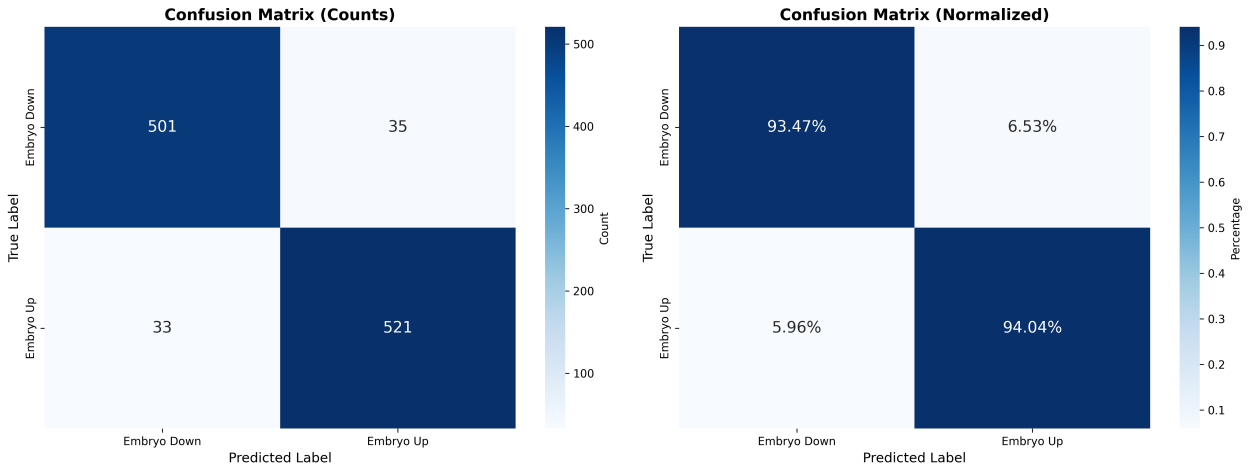


Figure 7: Confusion matrix for Stage 1, showing the distribution of true vs. predicted labels for the test set.

Compared to the CNN baselines, the CvT-based model improves absolute accuracy by roughly 7–17 percentage points and substantially increases F1 scores, highlighting the benefit of transformer-based global reasoning even for relatively simple binary tasks.

4.3 Stage 2—Shape Classification

Stage 2 receives pure kernels and predicts flat versus round morphology on a test set of 578 images. Table 7 reports the quantitative results, and the corresponding confusion matrix is shown in Figure 8. Accuracy improves slightly relative to Stage 1, and both shape classes show nearly identical F1 scores (≈ 0.94). Shape classification is inherently more subtle than gross impurity detection, as it primarily depends on global geometry and kernel silhouette. The high performance of Stage 2 indicates that the CvT backbone effectively captures

these morphological cues, supporting its suitability for shape-sensitive grading tasks.

This performance clearly surpasses the ResNet-50 and DenseNet-121 baselines, likely because those architectures are less effective at modeling the long-range spatial context required for accurate kernel shape analysis.

4.4 Stage 3—Embryo Orientation Classification

Stage 3 is the most challenging step: Given pure, flat kernels, it predicts whether the embryo is facing up or down. The test set contains 293 images. Table 8 shows per-class performance, and the corresponding confusion matrix is shown in Figure 9.

Despite the fine-grained nature of the task and the smaller sample size, Stage 3 achieves over 91% accuracy and macro F1 ≈ 0.91 . Embryo-up kernels are slightly easier to classify (higher Recall and F1),

Table 7: Classification report for Stage 2 (Flat vs. Round).

Class	Precision	Recall	F1 Score	Support
Flat	0.9362	0.9489	0.9425	294
Round	0.9464	0.9330	0.9396	284
Accuracy	—	—	0.9411	578
Macro avg	0.9413	0.9409	0.9410	578
Weighted avg	0.9413	0.9405	0.9413	578

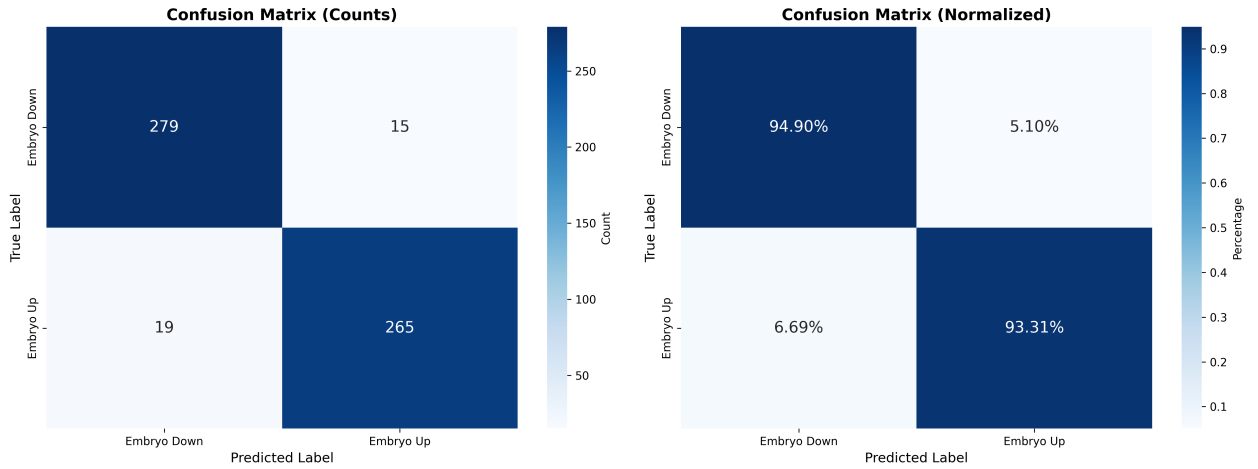


Figure 8: Confusion matrix for Stage 2, showing the distribution of true vs. predicted labels for the test set.

likely because embryo structures (e.g., scutellum, germ region) produce distinctive surface cues when facing the camera, whereas embryo-down kernels may resemble each other more subtly depending on lighting and angle.

The performance gap relative to the CNN baselines is even more pronounced here; CNNs find it difficult to distinguish such subtle orientation cues, whereas the CvT’s attention mechanisms appear to better capture global texture and shape patterns that signal orientation.

To summarize the comparative performance across all three stages, Table 9 reports test-set accuracies for CornViT and the two CNN baselines. CornViT achieves the highest accuracy in every stage, with gains of roughly 7 to 17 percentage points over ResNet-50 and about 2 to 7 percentage points over DenseNet-121.

4.5 Overall Pipeline Behavior and Error Propagation

Since the proposed framework, CornViT, is a hierarchical pipeline, errors in an early stage can propagate downstream. For example, a kernel misclassified as impure in Stage 1 will never be considered for shape or orientation analysis. However, the very high Stage 1 accuracy ($\approx 93.8\%$) limits the number of such cases.

One way to quantify end-to-end performance is to consider the effective accuracy for particularly important label combinations, such as “pure, flat, embryo up.” Assuming independence between stages, a rough lower bound on the probability of correctly classifying a kernel as pure, flat, and embryo up is

$$P(\text{correct all three}) \approx 0.9376 \times 0.9411 \times 0.9112 \approx 0.803.$$

This indicates that 80% of kernels that traverse all three stages could be classified correctly. In practice,

Table 8: Classification report for Stage 3 (Embryo up vs. Embryo down).

Class	Precision	Recall	F1 Score	Support
Embryo down	0.9043	0.8739	0.8890	119
Embryo up	0.9157	0.9367	0.9261	174
Accuracy	—	—	0.9112	293
Macro avg	0.9100	0.9053	0.9076	293
Weighted avg	0.9110	0.9102	0.9100	293

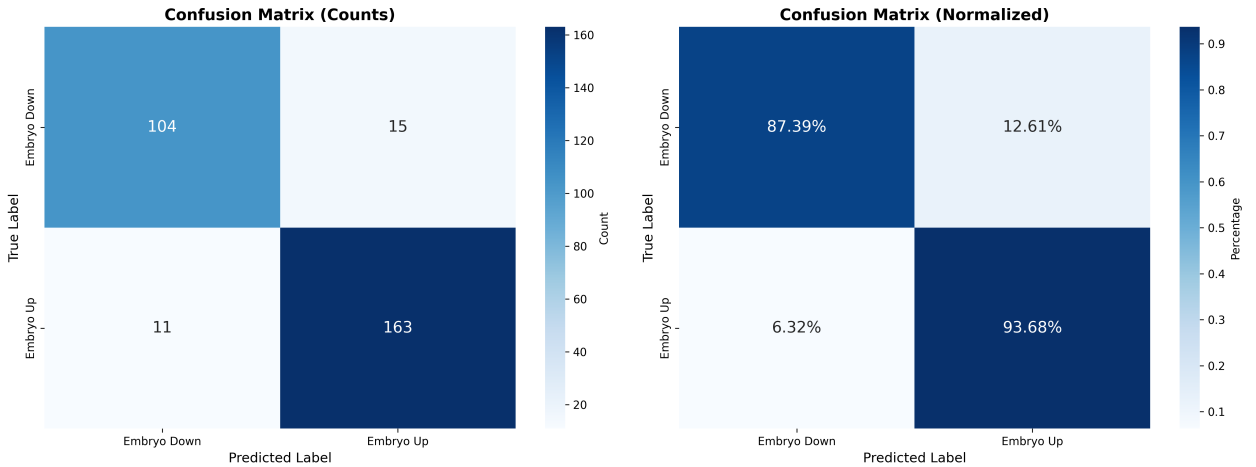


Figure 9: Confusion matrix for Stage 3, showing the distribution of true vs. predicted labels for the test set.

the true end-to-end accuracy depends on the distribution of samples and correlation of errors across stages. A more precise characterization of real-world performance would require a direct end-to-end evaluation of the complete three-stage pipeline on a joint test set covering all purity–shape–orientation combinations, which we leave for future work.

4.6 Visual Analysis

To complement the quantitative metrics reported so far, we performed qualitative visual analyses of CornViT’s predictions. Figure 10 illustrates representative examples from each stage, including both correctly and incorrectly classified kernels where y is the true label and \hat{y} is the predicted label.

For Stage 1, typical misclassifications involve borderline impurities: kernels that carry small artifacts such as tip cap (red/brown patch, point where the kernel was attached to the cob) or have slight devia-

tions from the idealized shape. These subtle irregularities can cause the model to hesitate or assign the wrong label. In Stage 2, errors are concentrated on kernels with intermediate shapes that lie between the “flat” and “round” prototypes. In Stage 3, the most challenging cases are kernels where the embryo is partially visible or where the embryo-facing side is only subtly different in appearance from the opposite side.

5 Web Application and System Integration

To make CornViT usable beyond the experimental setting, we implemented a ready-to-use web application that exposes the full hierarchical pipeline through a simple browser interface. This app is built with Python Flask (version 3.1.2) and bundles Aslam et al. (2015) all three trained CvT-13 mod-

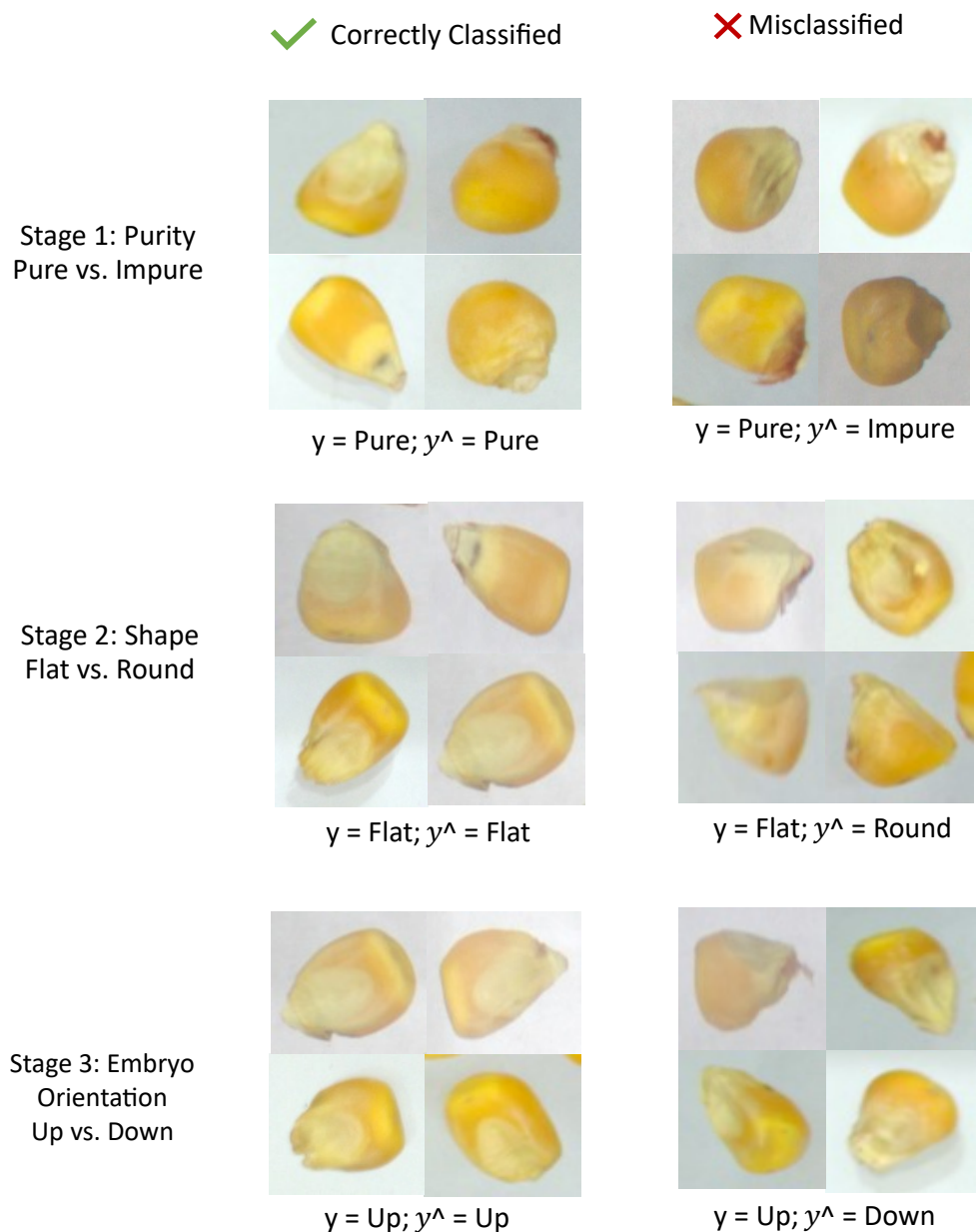


Figure 10: Representative CornViT predictions for each stage, including correctly classified and typical borderline misclassifications.

Table 9: Stage-wise comparison of CornViT and CNN baselines on the same test sets

Stage/Task	CornViT Acc.	ResNet-50 Acc.	DenseNet-121 Acc.
Stage 1 (purity)	93.76%	76.56%	86.56%
Stage 2 (shape)	94.11%	78.21%	87.05%
Stage 3 (embryo orientation)	91.12%	81.02%	89.38%

Algorithm 2 CornViT Hierarchical Inference

Require:

```

1:  $x_{\text{test}}$ : RGB image of a single kernel
2: Load trained models  $f_1, f_2, f_3$ 
3: val_transforms
4:  $x_1 \leftarrow \text{val\_transforms}(x_{\text{test}})$ 
5: Stage 1: Pure vs. Impure
6:  $\hat{y}_1 \leftarrow f_1(x_1)$ 
7: if  $\hat{y}_1$  = impure then
8:   Output: (impure,  $-$ ,  $-$ )
9:   return
10: end if
11: Stage 2: Flat vs. Round
12:  $x_2 \leftarrow x_1$ 
13:  $\hat{y}_2 \leftarrow f_2(x_2)$ 
14: if  $\hat{y}_2$  = round then
15:   Output: (pure, round,  $-$ )
16:   return
17: end if
18: Stage 3: Embryo Up vs. Down
19:  $x_3 \leftarrow x_2$ 
20:  $\hat{y}_3 \leftarrow f_3(x_3)$ 
21: Output: (pure, flat,  $\hat{y}_3$ )
  
```

els (purity, shape, embryo orientation) into a single end-to-end service.

5.1 Implementation

The system follows a standard client–server architecture. The client is implemented using HTML Pilgrim (2010), CSS Meyer (2006), JavaScript Crockford (2008), and provides a minimal interface that allows users to

- Upload a single RGB image of a corn kernel;
- Invoke the classification process with a single button click;
- Inspect stage-wise predictions and confidence scores.

The server-side backend is implemented in Flask and is responsible for the following:

- Loading the three CornViT models (Stage 1, 2, and 3) into memory at startup;
- Performing image validation and preprocessing;
- Orchestrating the hierarchical decision logic;
- Returning a structured JSON Pezoa et al. (2016) response to the client.

5.2 User Workflow and Visualization

From the user’s perspective, the workflow is illustrated as follows:

1. Open the CornViT web application in a browser (landing page, Figure 11).
2. Upload or drag-and-drop an image of a single kernel (Figure 12).
3. Click the “Analyze” button.
4. Inspect the stage-wise predictions and summary output returned by the system (Figures 13 and 14).
 - Stage 1: Impure vs. Pure with confidence.
 - Stage 2: Flat vs. Round (if pure) with confidence.
 - Stage 3: Embryo up vs. Embryo down (if pure and flat) with confidence.

For each stage, the interface displays both the predicted class and its associated confidence, together with the full pair of class probabilities: Impure/Pure for Stage 1, Flat/Round for Stage 2, and Embryo Up/Embryo Down for Stage 3.

The interface is minimal, allowing agronomists, seed technicians, and industry users to operate the system without prior knowledge of deep learning or Python internals.

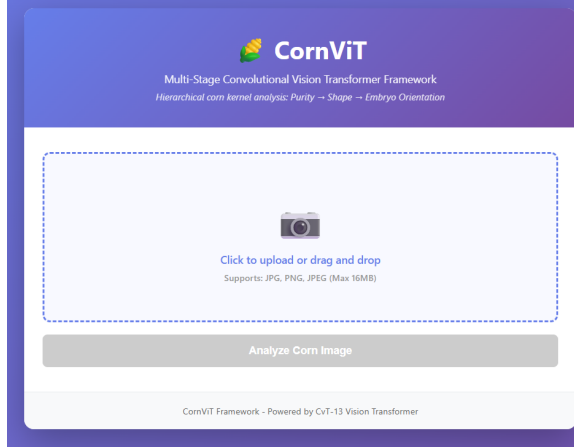


Figure 11: Landing page of the CornViT web interface.

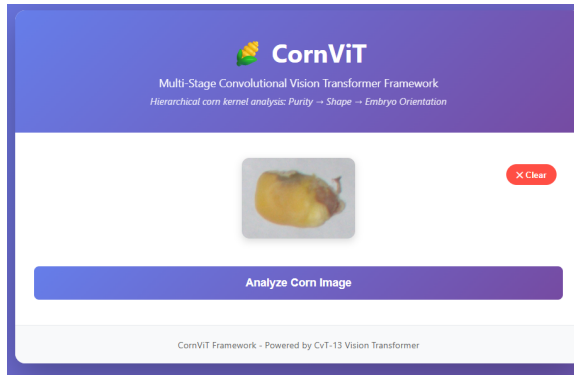


Figure 12: Screen showing the uploaded image and the analyze button.

5.3 Reproducibility and Deployment

The complete source code for the web application is publicly available at <https://github.com/SaiTeja-Erukude/CornViT-Client> (accessed on 19 December 2025). The app is designed in a loosely coupled manner and is distributed together with

1. The three trained CornViT model checkpoints (one for each stage);
2. The CvT-13 configuration files;
3. The preprocessing utilities and Flask routes.

This packaging allows straightforward deployment on a workstation or server running a recent Python

environment. The same codebase can be containerized (e.g., via Docker Anderson (2015)), providing a bridge from the experimental CornViT models to practical, day-to-day kernel quality assessment. Users may also substitute their own models while reusing the web application as a model-agnostic service.

6 Discussion

The results demonstrate that the proposed CornViT framework can reliably reproduce human-style hierarchical reasoning for corn kernel grading. Across all three stages, the CvT-13 backbone paired with stage-specific binary heads achieved high and well-balanced performance, with accuracies exceeding 91%. This indicates that the combination of convolutional token embedding and convolutional self-attention projections provides a strong inductive bias for capturing both local texture and global morphology in kernel images.

A first observation is that the hierarchical design is both effective and practical. Rather than forcing the model to infer a composite label in a single step, CornViT decomposes grading into three interpretable decisions: whether the kernel is pure, what its gross shape is, and, for pure-flat kernels, how the embryo is oriented. Each decision aligns with a question human graders routinely ask, making the intermediate outputs meaningful in their own right. The high and symmetric Precision–Recall values in Stages 1 and 2 suggest that these initial filters are robust, providing a stable foundation for more subtle orientation analysis in Stage 3.

The comparison with CNN baselines further highlights the benefits of transformer-based backbones in this domain. Under identical training conditions, CornViT consistently outperforms strong CNN architectures such as ResNet-50 and DenseNet-121 across all stages, with the largest gains observed in the embryo-orientation task, where discrimination depends on subtle cues in kernel surface structure and silhouette. The results suggest that convolution-augmented self-attention is especially well-suited to tasks that combine fine-grained texture analysis with global shape reasoning.

The stage-wise dataset design also plays a crucial role. By constructing separate, carefully curated datasets for purity, shape, and embryo orientation,

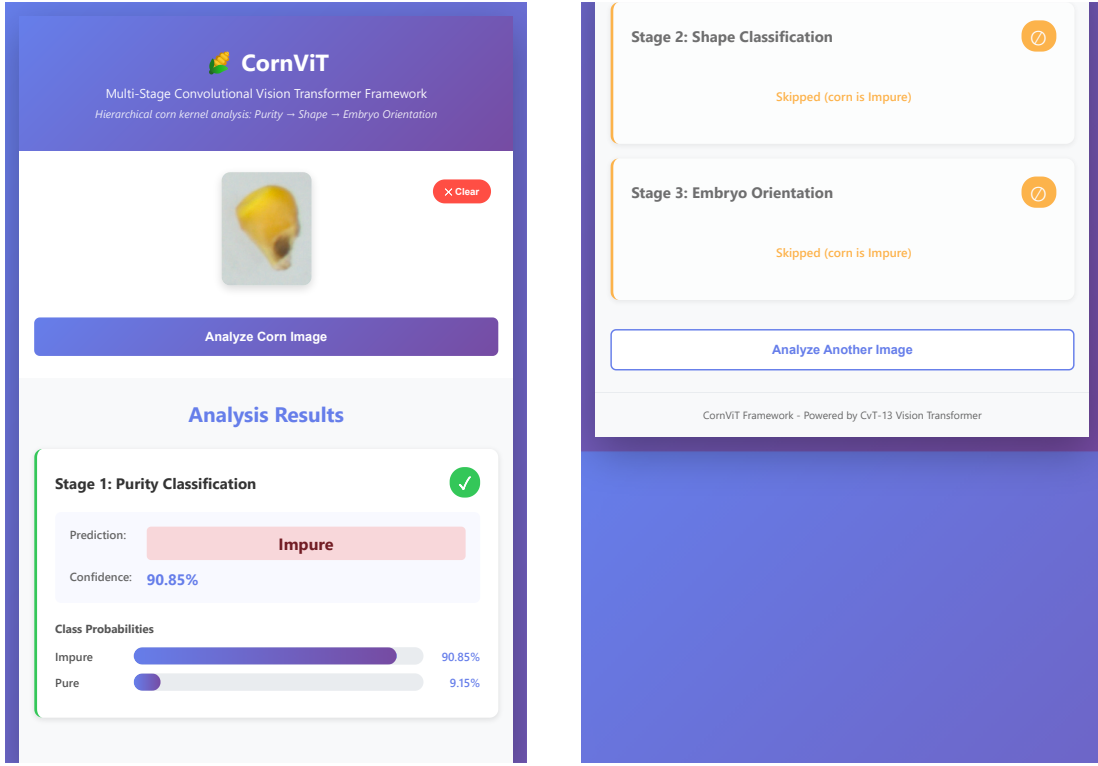


Figure 13: Example CornViT web-app result for an impure kernel. Stage 1 predicts Impure with high confidence, and the interface explicitly shows the corresponding class probabilities (Impure vs. Pure). Because the kernel is impure, Stages 2 (shape) and 3 (embryo orientation) are skipped and marked as not applicable.

we avoid conflating label noise in the original source with model capacity. Each stage can be trained and evaluated on labels tailored to its specific decision, enabling a cleaner analysis of model behavior and error modes. At the same time, the three datasets can be reassembled to study error propagation in the full pipeline, e.g., how misclassifications in Stage 1 affect downstream shape and orientation predictions.

From a deployment perspective, the hierarchical structure and the accompanying Flask-based web application make the system attractive for practical seed quality workflows. The web interface exposes stage-wise predictions and confidences through a simple browser front-end, lowering the barrier to adoption for agronomists and seed technicians who may not be familiar with deep learning frameworks.

The ability to skip later stages when a kernel is clearly impure also saves computation in potential high-throughput settings.

Beyond corn kernels, CornViT fits into a broader trend toward automated, image-based classification of agricultural products. Similar hierarchical pipelines could be designed for fruit or vegetable grading (e.g., separating healthy from damaged fruit before finer defect categorization) or for multi-stage assessment of silage quality, where stages might reflect purity, particle-size characteristics, and kernel processing score. In this sense, CornViT complements recent work such as Succulent-YOLO Li et al. (2025), which uses a modern YOLO-based pipeline with CLIP-enhanced features for agricultural product classification from UAV imagery, and the 2022 study on real-time estimation of corn silage ker-

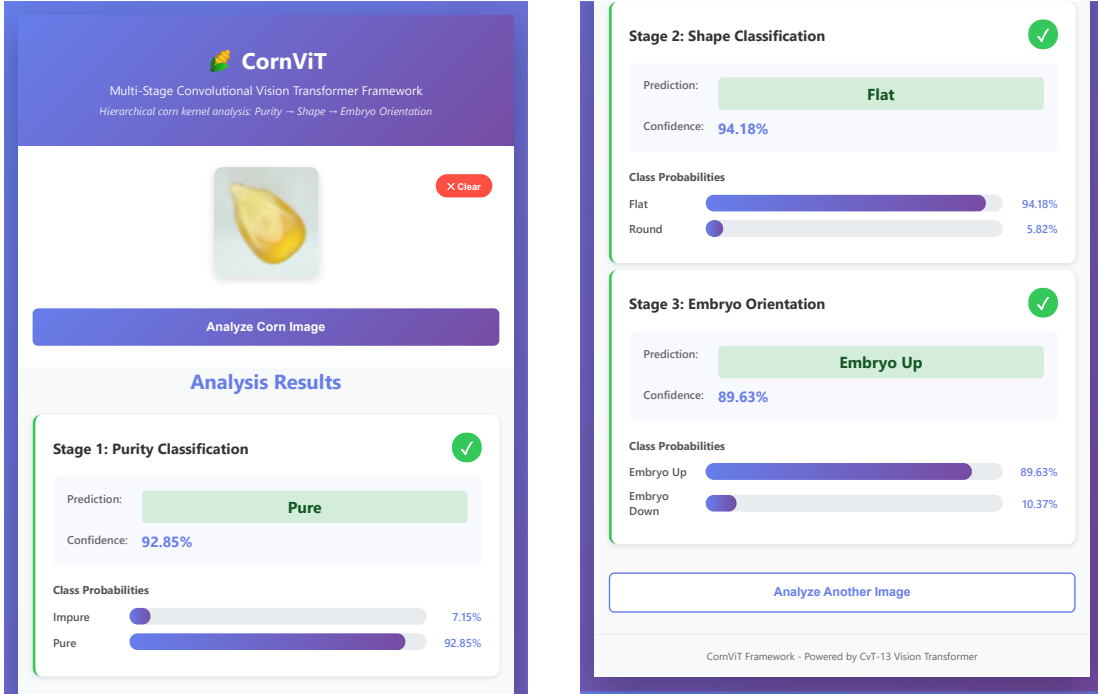


Figure 14: Example CornViT web-app result for a pure-flat kernel with the embryo facing up. Stage 1 predicts Pure with high confidence; Stage 2 then classifies the kernel as Flat and displays probabilities for the Flat and Round classes; Stage 3 finally predicts Embryo Up and provides probabilities for the Embryo Up and Embryo Down classes. All three stages are executed.

nel processing score from image data Rocha et al. (2022), both of which demonstrate how deep learning can support decision-making across the crop production chain.

At the same time, several limitations merit discussion. First, the imaging setup is relatively controlled, with a single general style of background, lighting, and camera placement. The extent to which CornViT generalizes to other cameras, lighting conditions, or varieties remains to be fully explored. Second, the current model operates on single kernels placed on a uniform background; extending the approach to multi-kernel scenes or conveyor-belt imagery would require additional detection or segmentation modules. Third, the independence

assumption used in our rough joint-accuracy estimate may not hold perfectly in practice, as errors across stages can be correlated. Finally, although head-only fine-tuning is computationally efficient and performed well here, it constrains the model’s ability to adapt to the fine-grained visual differences that drive the Stage 3 embryo-orientation decision. More flexible strategies, such as selectively unfreezing the final CvT stage, applying layer-wise learning-rate decay, could enable the model to better capture subtle structural cues associated with embryo position.

Future work will investigate several directions, including progressive unfreezing and low-rank adaptation (LoRA), as alternatives that balance stability

with representational flexibility. They will also examine joint multi-task training with a shared backbone and multiple heads, which may improve parameter efficiency and exploit shared structure across stages. Domain adaptation and data augmentation strategies could be explored to improve robustness to new imaging setups and additional corn varieties. Incorporating attention or saliency visualizations directly into the web interface may further enhance interpretability for end users. Finally, extending the hierarchical framework to other crop species and quality attributes such as damage, disease, or varietal classification could broaden its relevance to precision agriculture and seed-processing pipelines.

7 Conclusions

This paper presented CornViT, a multi-stage Convolutional Vision Transformer framework for hierarchical corn kernel analysis. By explicitly mirroring the reasoning process of human seed analysts through three sequential decisions: purity (impure vs. pure), shape (flat vs. round), and embryo orientation (up vs. down), CornViT delivers accurate and interpretable kernel-level grading from RGB images. Across dedicated test sets, the three CvT-13 models achieved stage-wise accuracies of 93.76%, 94.11%, and 91.12%, respectively, with strong per-class F1 scores, including for the more challenging embryo-orientation task.

Compared with strong CNN baselines, CornViT consistently delivers higher stage-wise performance, underscoring the benefits of convolution-augmented self-attention for capturing global morphology and subtle surface cues within a hierarchical decision framework.

A further contribution of this work is the construction of a ready-to-use, stage-wise annotated dataset tailored to hierarchical kernel classification. Each image is labeled for purity, morphology, and, where applicable, embryo orientation, enabling both isolated stage-wise training and end-to-end pipeline evaluation. Together with the curated datasets, the lightweight Flask-based web application that encapsulates the full CornViT pipeline makes the approach readily deployable in laboratory and industrial environments.

Future research directions include investigating progressive unfreezing, joint multi-task training of

a shared backbone, exploring more advanced fine-tuning strategies, and improving robustness to diverse imaging conditions and corn varieties. Extending the framework to multi-kernel scenes, conveyor-based inspection, and other crop species would further enhance its impact on smart seed processing and precision agriculture. Overall, the CornViT framework and accompanying dataset provide a solid foundation for accurate, interpretable, and deployable seed- and kernel-level quality control systems.

References

Anderson, C. (2015). Docker [software engineering]. *IEEE software*, 32(3):102–c3.

Aslam, F. A., Mohammed, H. N., and Lokhande, P. S. (2015). Efficient way of web development using python and flask. *International Journal of Advanced Research in Computer Science*, 6(2).

Bai, H., Wang, N., and Long, J. (2024). Image-based corn seed embryo orientation detection and adjustment for precision planting. *Computers and Electronics in Agriculture*, 224:109139.

Barman, U., Sarma, P., Rahman, M., Deka, V., Lahkar, S., Sharma, V., and Saikia, M. J. (2024). Vit-smartagri: vision transformer and smartphone-based plant disease detection for smart agriculture. *Agronomy*, 14(2):327.

Changqing, L., Bingqi, C., Xinhui, Z., Qiao, W., and Xi, Y. (2015). Dynamic detection of corn seeds for directional precision seeding. *Nongye Jixie Xuebao/Transactions of the Chinese Society of Agricultural Machinery*, 46(9).

Chen, T., Kornblith, S., Norouzi, M., and Hinton, G. (2020). A simple framework for contrastive learning of visual representations. In *International conference on machine learning*, pages 1597–1607. PMLR.

Crockford, D. (2008). *JavaScript: The Good Parts: The Good Parts*. ” O'Reilly Media, Inc.”.

De Silva, M. and Brown, D. (2023). Multispectral plant disease detection with vision transformer-convolutional neural network hybrid approaches. *Sensors*, 23(20):8531.

Dong, D., Nagasubramanian, K., Wang, R., Frei, U. K., Jubery, T. Z., Lübbertedt, T., and Ganapathysubramanian, B. (2023). Self-supervised maize kernel classification and segmentation for embryo identification. *Frontiers in Plant Science*, Volume 14 - 2023.

Dosovitskiy, A. (2020). An image is worth 16x16 words: Transformers for image recognition at scale. *arXiv preprint arXiv:2010.11929*.

Fortin, M.-C. and Pierce, F. (1996). Leaf azimuth in strip-intercropped corn. *Agronomy Journal*, 88(1):6–9.

Ghaffari, A. (2024). Precision seed certification through machine learning. *Technology in Agronomy*, 4(tia-0024-0013).

Gomroki, M., Benaragama, D., Henry, C. J., Badreldin, N., and Gulden, R. (2025). Cwrepvitnet: An encoder-decoder deep learning framework with repvit blocks for crop weed semantic segmentation in soybean fields through their life journey. *Smart Agricultural Technology*, 12:101472.

Hammouda, K., Khalifa, F., Alghamdi, N. S., Darwish, H., and El-Baz, A. (2022). Multi-stage classification-based deep learning for gleason system grading using histopathological images. *Cancers*, 14(23):5897.

Hasasneh, A., Ghannam, R., and Masri, S. (2025). Weednet-vit: A vision transformer approach for robust weed classification in smart farming. *Geographies*, 5(4):64.

He, K., Zhang, X., Ren, S., and Sun, J. (2016). Deep residual learning for image recognition. In *Proceedings of the IEEE conference on computer vision and pattern recognition*, pages 770–778.

Huang, G., Liu, Z., Van Der Maaten, L., and Weinberger, K. Q. (2017). Densely connected convolutional networks. In *Proceedings of the IEEE conference on computer vision and pattern recognition*, pages 4700–4708.

Juba, B. and Le, H. S. (2019). Precision-recall versus accuracy and the role of large data sets. In *Proceedings of the AAAI conference on artificial intelligence*, volume 33, pages 4039–4048.

Koonce, B. (2021). Resnet 50. In *Convolutional neural networks with swift for tensorflow: image recognition and dataset categorization*, pages 63–72. Springer.

LeCun, Y., Bengio, Y., and Hinton, G. (2015). Deep learning. *nature*, 521(7553):436–444.

Li, G., Wang, Y., Zhao, Q., Yuan, P., and Chang, B. (2023). Pmv: a lightweight vision transformer for plant disease identification on mobile devices. *Frontiers in Plant Science*, 14:1256773.

Li, H., Zhao, F., Xue, F., Wang, J., Liu, Y., Chen, Y., Wu, Q., Tao, J., Zhang, G., Xi, D., Chen, J., and Kobayashi, H. H. (2025). Succulent-yolo: Smart uav-assisted succulent farmland monitoring with clip-based yolov10 and mamba computer vision. *Remote Sensing*, 17(13).

Liao, K., Paulsen, M. R., Reid, J. F., Ni, B. C., and Bonifacio-Maghirang, E. P. (1993). Corn kernel breakage classification by machine vision using a neural network classifier. *Transactions of the ASAE*, 36(6):1949–1953.

Loshchilov, I. and Hutter, F. (2017). Decoupled weight decay regularization. *arXiv preprint arXiv:1711.05101*.

Meyer, E. A. (2006). *CSS: The Definitive Guide: The Definitive Guide.* ” O'Reilly Media, Inc.”.

Nehoshtan, Y., Carmon, E., Yaniv, O., Ayal, S., and Rotem, O. (2021). Robust seed germination prediction using deep learning and rgb image data. *Scientific Reports*, 11(1):22030.

O'shea, K. and Nash, R. (2015). An introduction to convolutional neural networks. *arXiv preprint arXiv:1511.08458*.

Parez, S., Dilshad, N., Alghamdi, N. S., Alanazi, T. M., and Lee, J. W. (2023). Visual intelligence in precision agriculture: Exploring plant disease detection via efficient vision transformers. *Sensors*, 23(15):6949.

Paszke, A., Gross, S., Massa, F., Lerer, A., Bradbury, J., Chanan, G., Killeen, T., Lin, Z., Gimelshein, N., Antiga, L., et al. (2019). Pytorch: An imperative style, high-performance deep learning library. *Advances in neural information processing systems*, 32.

Peters, D. and Woolley, J. (1959). Orientation planting means more moisture. *Agricultural Research*, 7(9):6–7.

Pezoa, F., Reutter, J. L., Suarez, F., Ugarte, M., and Vrgoč, D. (2016). Foundations of json schema. In *Proceedings of the 25th international conference on World Wide Web*, pages 263–273.

Pilgrim, M. (2010). *HTML5: up and running: dive into the future of web development.* ” O'Reilly Media, Inc.”.

Qin, R., Chai, H. K., Liu, K., Yu, H., and Huang, J. (2025). A hierarchical multi-stage fusion deep learning framework for short-term wind power prediction. *Renewable Energy*, page 123551.

Rocha, E. M., Drewry, J. L., Willett, R. M., and Luck, B. D. (2022). Assessing kernel processing score of harvested corn silage in real-time using image analysis and machine learning. *Computers and Electronics in Agriculture*, 203:107415.

sethu123123 (2025). cornseed. <https://www.kaggle.com/datasets/sethu123123/cornseed>. Accessed: 2025-11-20.

Sonka, M., Hlavac, V., and Boyle, R. (2013). *Image processing, analysis and machine vision*. Springer.

Surse, M. and Yawalkar, P. (2025). Automated evaluation of onion seed quality using physical characteristics via image processing and machine learning techniques. *Org. Farming*, 11(1):39–48.

Toler, J., Murdock, E., Stapleton, G., and Wallace, S. (1999). Corn leaf orientation effects on light interception, intraspecific competition, and grain yields. *Journal of production agriculture*, 12(3):396–399.

Torres, G., Vossenkemper, J., Raun, W., and Taylor, R. (2011). Maize (zea mays) leaf angle and emergence as affected by seed orientation at planting. *Experimental Agriculture*, 47(4):579–592.

Velesaca, H. O., Mira, R., Suárez, P. L., Larrea, C. X., and Sappa, A. D. (2020). Deep learning based corn kernel classification. *2020 IEEE/CVF Conference on Computer Vision and Pattern Recognition Workshops (CVPRW)*, pages 294–302.

Wang, Y., Xu, L., Zhao, X., and Hou, X. (2014). Maize seed embryo and position inspection based on image processing. *Computer and Computing Technologies in Agriculture VII*, pages 1–9.

Wu, H., Xiao, B., Codella, N., Liu, M., Dai, X., Yuan, L., and Zhang, L. (2021a). CvT-13 imagenet-22k pretrained checkpoint. <https://onedrive.live.com/?id=56B9F9C97F261712%2115004&cid=56B9F9C97F261712&redee=aHR0cHM6Ly8xZHJ2Lm1zL3UvcyFBaElYSm5fSi1ibFc5UnpGM3> Pretrained weights for CvT-13 on ImageNet-22k.

Wu, H., Xiao, B., Codella, N., Liu, M., Dai, X., Yuan, L., and Zhang, L. (2021b). CvT: Introducing convolutions to vision transformers.

Wu, H., Xiao, B., Codella, N., Liu, M., Dai, X., Yuan, L., and Zhang, L. (2021c). microsoft/cvt: Official implementation of cvt – introducing convolutions to vision transformers. <https://github.com/microsoft/CvT>. GitHub repository, MIT License.

Zhang, M., Liu, C., Li, Z., and Yin, B. (2025). From convolutional networks to vision transformers: Evolution of deep learning in agricultural pest and disease identification. *Agronomy*, 15(5):1079.

Zhou, S., Chai, X., Yang, Z., et al. (2021). Maize-ias: a maize image analysis software using deep learning for high-throughput plant phenotyping. *Plant Methods*, 17(48).

Zhu, Q., Liu, Q., Ma, D., Zhu, Y., Zhang, L., Wang, A., and Fan, S. (2025). Maize seed variety classification based on hyperspectral imaging and a cnn-lstm learning framework. *Agronomy*, 15:1585.